

# Truly bulk-sensitive spectroscopic measurements of valence in heavy fermion materials†

Claudia Dallera,<sup>a\*</sup> Marco Grioni,<sup>b</sup> Abhay Shukla,<sup>c</sup> Gyorgy Vankò<sup>c</sup> and John L. Sarrao<sup>d</sup>

<sup>a</sup>INFM - Dipartimento di Fisica, Politecnico di Milano, I-20133 Milano, Italy, <sup>b</sup>Ecole Polytechnique Fédérale (EPFL), CH-1015 Lausanne, Switzerland, <sup>c</sup>European Synchrotron Radiation Facility, BP 220, Grenoble, France, and <sup>d</sup>Los Alamos National Laboratory, Los Alamos, NM 87545, USA.  
E-mail: claudia.dallera@fisi.polimi.it

Intermediate valence is one of the typical phenomena of systems with strong electronic correlation. The Anderson impurity model predicts a scaling of the valence with the reduced temperature  $T/T_K$ , which is difficult to observe by traditional surface-sensitive electronic spectroscopies. This paper presents results obtained by resonant inelastic X-ray scattering (RIXS), a bulk-sensitive configuration- and chemical-specific technique. The temperature dependence of the valence of YbInCu<sub>4</sub> and YbAgCu<sub>4</sub> was measured by tuning the incident energy to the resonance of the Yb<sup>2+</sup> spectral component. In the case of YbInCu<sub>4</sub> a sharp valence transition, as known from thermodynamical measurements, has been found. The valence of YbAgCu<sub>4</sub> reveals a smooth dependence consistent with a Kondo temperature  $T_K = 70$  K. These findings establish RIXS as a powerful tool for measuring bulk electronic properties of solids.

**Keywords:** mixed valence; RIXS; heavy fermions; Kondo behaviour; ytterbium; rare earths; Anderson impurity model.

## 1. Introduction

Mixed valence arises in strongly correlated solids from the conflict between the natural tendency of electrons to form extended bands and the opposite tendency to occupy atomic-like localized states. This leads to spectacular physical properties including Kondo and heavy fermion behaviour as well as unconventional magnetism and superconductivity (Lee *et al.*, 1986).

Valence fluctuations can be revealed by various transport, thermodynamic and spectroscopic measurements. The latter probe, in the most direct way, the nature of the electronic ground state but typically only sample a thin layer ( $\sim 10\text{--}20$  Å) below the surface. Recent experiments at higher photon energy (Sekiyama *et al.*, 1997; Braicovich *et al.*, 1997) with larger probing ranges ( $\sim 20\text{--}50$  Å) highlight the limitations of conventional measurements. This disadvantage is overcome by photon in–photon out spectroscopies like resonant inelastic X-ray scattering (RIXS), which probes the electronic states of a much thicker ( $\sim 10$  μm in our experiment) bulk-like layer. RIXS is also element-specific and can distinguish between different electronic configurations. These characteristics make RIXS an ideal tool to obtain bulk information about intermediate-valence systems, as we prove in the present study of valence in the two Yb-based Kondo systems YbInCu<sub>4</sub> and YbAgCu<sub>4</sub>. The valence is predicted by the Anderson impurity model (AIM) to scale with the reduced temperature  $T/T_K$ , where  $T_K$  is the Kondo temperature

(Bickers *et al.*, 1987). YbInCu<sub>4</sub>, a moderately heavy fermion, was chosen as a model compound. It exhibits a first-order transition at  $T_V = 42$  K, where the valence suddenly decreases from 2.96 to 2.83, and  $T_K$  changes from  $\sim 20$  K to  $\sim 400$  K. Such a small valence difference gives rise to large changes in all the physical properties. For YbAgCu<sub>4</sub>, a smooth transition with temperature is expected, consistent with  $T_K \simeq 60\text{--}100$  K. The mentioned valence changes have been hinted at by a wealth of non-spectroscopic measurements. Spectroscopic results in these and in related Kondo systems are controversial, due to possible contributions from perturbed surface layers (Malterre *et al.*, 1997). The present findings unambiguously demonstrate the validity of the AIM predictions providing results that are related to truly bulk states.

## 2. Experimental

The experiment was performed on the ESRF beamline ID16. The incident radiation was monochromated by an Si(111) monochromator. X-rays scattered at 90° by the sample were energy-analyzed with a Rowland circle-based spectrometer equipped with a silicon crystal cut along the (620) direction. We measured  $L\alpha_1$  ( $3d\text{--}2p$ ) RIXS spectra of ytterbium at selected excitation energies across the  $L_3$  ( $2p_{3/2}$ ) threshold, and  $L_3$  absorption spectra (XAS) by recording the intensity of the  $L\alpha_1$  fluorescence while scanning the incident photon energy. These partial fluorescence yield (PFY) spectra are free from the lifetime broadening of the deep core-hole (Hämäläinen *et al.*, 1991). The overall resolution was 1.3 eV. The samples were polished single crystals mounted on an He closed-cycle refrigerator allowing accurate temperature control between 15 K and 300 K.

## 3. Results and discussion

The ground state of ytterbium in YbInCu<sub>4</sub> and YbAgCu<sub>4</sub> is a coherent superposition of Yb<sup>2+</sup> ( $4f^{14}$ ) and Yb<sup>3+</sup> ( $4f^{13}$ ) states. Fig. 1 shows the electronic configuration of ytterbium in the ground state and in the intermediate and final states of the RIXS process, together with the main transitions connecting the different configurations. The fingerprints of both Yb<sup>2+</sup> ( $4f^{14}$ ) and Yb<sup>3+</sup> ( $4f^{13}$ ) are visible in the Yb  $L_3$  PFY spectra of YbInCu<sub>4</sub>, recorded below and above the transition temperature (Fig. 2). The intensity of the Yb<sup>2+</sup> component drops at  $T_V$ , reflecting the sudden change of valence. For comparison we show the same absorption spectra measured in the traditional total fluorescence yield mode. These results are consistent with previous data

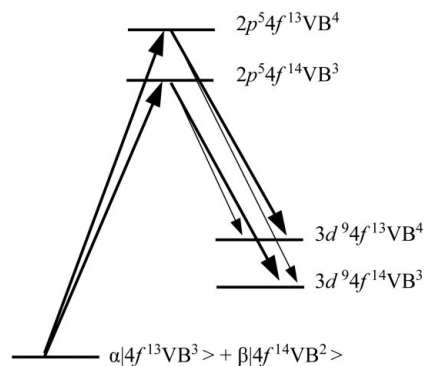


**Figure 1**  
Total energy level scheme for a Yb ion in mixed-valent ytterbium compounds. The arrows indicate the relevant XAS and RIXS transitions. The XAS final states are the intermediate states of the RIXS process.

† Presented at the ‘International Workshop on High-Resolution Photoemission Spectroscopy of Correlated Electron Systems’ held at Osaka, Japan, in January 2002.

(Cornelius *et al.*, 1997) but the use of the PFY detection results in superior resolution and much better defined spectral features.

The quantitative determination of the  $\text{Yb}^{2+}$  weight in the ground state is necessary to evaluate the deviation from the integer 3+ valence. The corresponding XAS signal is small. However, the sensitivity to the divalent configuration can be greatly enhanced by tuning the excitation energy to the peak of the  $\text{Yb}^{2+}$  XAS signal and recording the corresponding RIXS spectrum. This is clearly illustrated by Fig. 3, showing RIXS spectra collected at various energies around the  $\text{Yb}^{2+}$  resonance. At the peak of the resonance the  $\text{Yb}^{2+}$  signal dominates the spectrum for  $T = 15$  K (below the transition). Above the transition temperature ytterbium is closer to trivalent, and the divalent contribution is less intense.

The temperature dependence of the divalent signal is most clearly observed at resonance. Fig. 4 shows the change of the spectral shape for both compounds. The small valence changes yield large changes in the weight of the divalent component, which is proportional to  $(1 - n_h)$ , where  $n_h$  is the number of  $f$ -holes ( $n_h = 0$  for  $\text{Yb}^{2+}$ ,  $n_h = 1$  for  $\text{Yb}^{3+}$ ). The spectra of  $\text{YbInCu}_4$  exhibit a variation only across  $T_V$ . For  $\text{YbAgCu}_4$  the line shape changes continuously between the two extreme cases of Fig. 4. The temperature dependence was followed continuously by monitoring the divalent peak intensity (shaded region in Fig. 4). The measured intensity was corrected to account for the overlapping tail of the trivalent signal, determined from the fluorescence spectrum excited 30 eV above the absorption threshold (dashed line).

The temperature evolution of the divalent component is presented in Fig. 5. The measured intensities have been converted into absolute  $(1 - n_h)$  values by using the low-temperature  $n_h$  values of Lawrence *et al.* (1994) (0.83 for  $\text{YbInCu}_4$  and 0.87 for  $\text{YbAgCu}_4$ ). A very different behaviour with temperature is identified: in  $\text{YbInCu}_4$  the edge

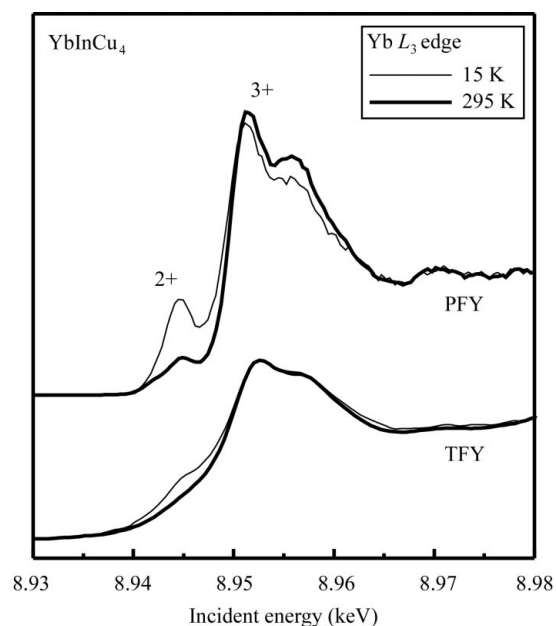


**Figure 2**

Ytterbium  $L_3$  absorption spectrum in  $\text{YbInCu}_4$  measured on the same sample in partial fluorescence yield (PFY) mode (top) and in conventional total fluorescence yield (TFY) mode (bottom). In the PFY mode only the emitted radiation corresponding to  $3d_{5/2}-2p_{3/2}$  decay ( $h\nu_{\text{out}} = 7415$  eV) was recorded. The spectra exhibit features corresponding to the 2+ and 3+ configurations in the initial state. Their intensity change across the transition temperature ( $T_V = 42$  K) reflects the valence change.

located around  $T_V = 42$  K reveals the sudden valence change at the transition temperature. In  $\text{YbAgCu}_4$  the evolution is smooth and exhibits a concavity change around 70 K. The dashed curve is the prediction of the AIM, calculated within the non-crossing approximation (NCA), assuming a Kondo temperature  $T_K = 70$  K.

RIXS data at the  $L$  edges of rare earths contain a further independent indicator of valence. In fact, in addition to the dipolar  $2p-5d$  transition, a  $2p-4f$  quadrupolar excitation is also possible in the absorption step of the scattering process. The quadrupolar transition is much weaker than the dipolar one and is detected only for excitation energies well below the  $2p-5d$  absorption threshold (Dallera *et al.*, 2000). Nonetheless, this channel is very interesting because it directly involves the  $4f$  states. This transition is therefore a very powerful indicator of rare-earth valence changes driven by external temperature and pressure conditions, especially in Yb, where the  $4f$  shell is close to being filled. The quadrupolar transition cannot occur in divalent ( $4f^{14}$ ) metallic ytterbium. In compounds, following hybridization with the  $5d$  orbitals,  $n_h$  holes are available for the transition. The quadrupolar feature is indicated by the arrows in Fig. 6, displaying spectra excited at the resonance of the  $2p-4f$  tran-

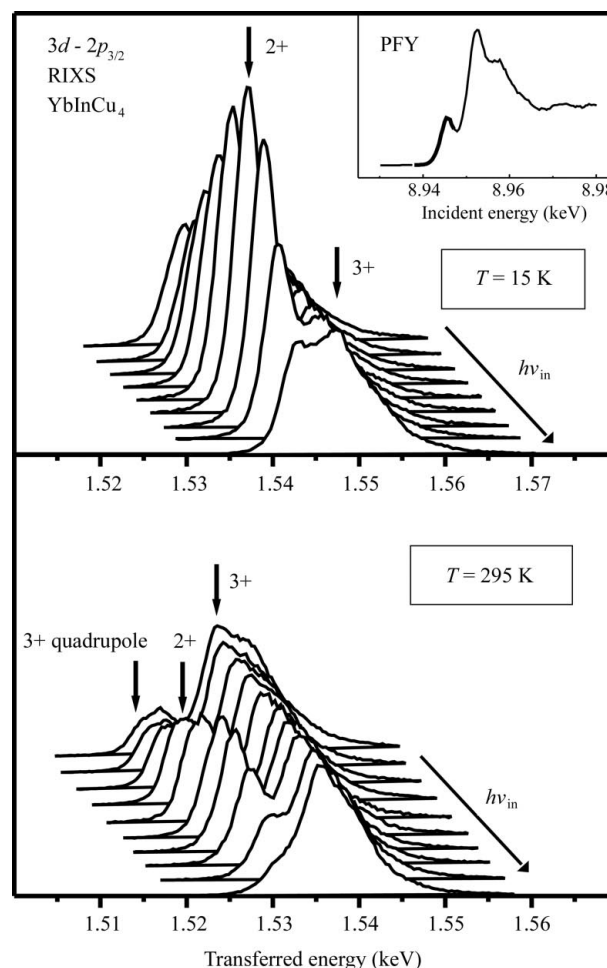


**Figure 3**

RIXS spectra of ytterbium in  $\text{YbInCu}_4$ . The incident energy was scanned in the region of the  $\text{Yb}^{2+}$  signal (thick part of absorption curve in the inset). At its resonance peak is the most prominent spectral feature below  $T_V$  ( $T = 15$  K). Above  $T_V$  ( $T = 295$  K) the Yb valence is closer to 3 and the divalent peak is less intense. At this temperature the weak contribution from the intermediate state following  $2p-4f$  quadrupolar excitation is observed (see Fig. 6 for more details).

sition. It appears at a lower energy transfer because the addition of an electron into the  $4f$  states leaves the system in a less excited state. The peak is evident at high temperature when ytterbium is in an almost trivalent state. At low temperature it appears only as a shoulder. Both the dipolar and quadrupolar features carry in principle the same

information on the Yb valence state. However, since the dipolar channel involves extended conduction states, a quantitative comparison of their relative intensities is not straightforward and should explicitly take into account the material-dependent  $5d$  density of states near  $E_F$ , and subtle details of the resonance profile.

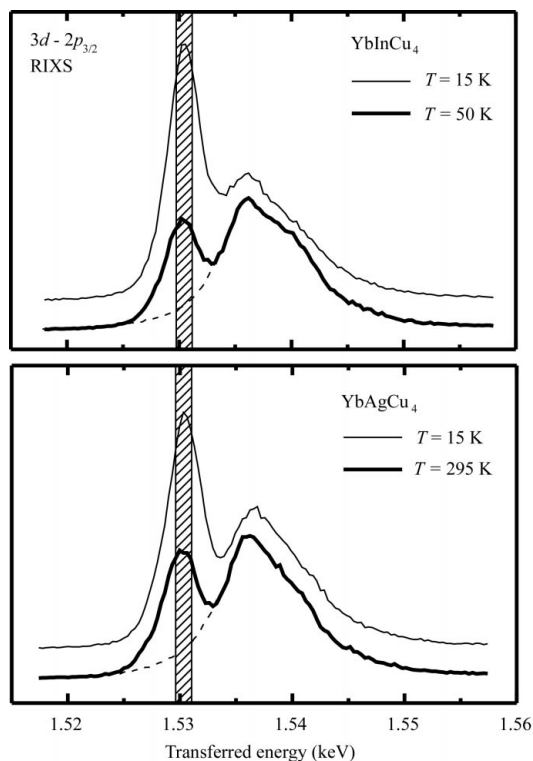


**Figure 4**  
Yb  $L\alpha_1$  RIXS spectra in YbInCu<sub>4</sub> and YbAgCu<sub>4</sub> excited at the maximum of the Yb<sup>2+</sup> resonance. The small change of valence with temperature ( $\Delta n_f = 0.13$  for YbInCu<sub>4</sub> and 0.065 for YbAgCu<sub>4</sub>) results in a large change of the divalent peak intensity. The shaded area indicates the spectral region whose intensity was monitored *versus* temperature. The dashed line is the fluorescent contribution that was subtracted from the RIXS spectra to estimate the intensity of the divalent component (shown in Fig. 5).

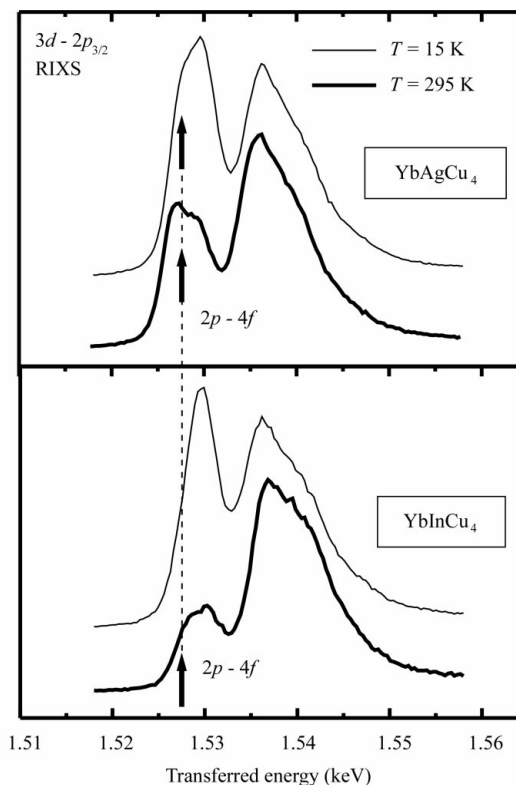


**Figure 6**  
When the excitation energy is tuned below the  $2p-5d$  dipolar excitation threshold the intensity of the quadrupolar  $2p-4f$  transition is enhanced. The arrows point to the RIXS peak following quadrupolar excitation ( $h\nu_{in} = 8940$  eV). This feature is well seen at high temperature, where both compounds are close to the trivalent configuration. At low temperature the quadrupolar feature is seen as a weak shoulder.

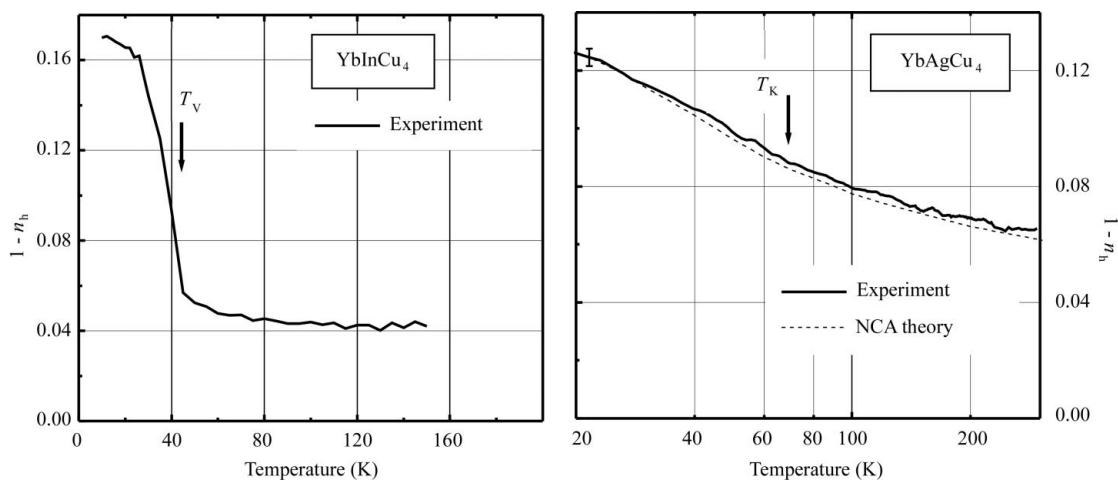


**Figure 5**  
The continuous intensity evolution of the divalent RIXS signal has been converted into  $1 - n_h$  values ( $n_h =$  number of  $f$ -holes) by adopting the XAS value  $n_h = 0.83$  for YbInCu<sub>4</sub>, and 0.87 for YbAgCu<sub>4</sub>. YbInCu<sub>4</sub> shows a sharp transition. The evolution of YbAgCu<sub>4</sub> agrees with the NCA calculation for  $T_K = 70$  K (dashed curve).

The present results confirm that the Anderson model provides a sound theoretical framework also for the spectral properties of Kondo systems. Previous inconsistencies are most likely due to the short probing depth of electron spectroscopies, and to perturbed surface layers. They demonstrate that RIXS is an extremely interesting bulk probe of intermediate valence thanks to the possibility of resonantly enhancing the contribution of a specific electronic configuration of interest. Extensions to other strongly correlated systems like the transition metal oxides, and to experiments under pressure or in external fields, which are precluded to electron spectroscopies, are being considered.

We would like to thank M. H. Krisch and J. P. Rueff for assistance and discussion in the preliminary stage of the experiment. CD is indebted to R. Montegue for invaluable support.

## References

- Bickers, N. E., Cox, D. L. & Wilkins, J. W. (1987). *Phys. Rev. B*, **36**, 2036–2079.
- Braicovich, L., Brookes, N. B., Dallera, C., Salvietti, M. & Olcese, G. L. (1997). *Phys. Rev. B*, **56**, 15047–15055.
- Cornelius, A. L., Lawrence, J. M., Sarrao, J. L., Fisk, Z., Hundley, M. F., Kwei, G. H., Thompson, J. D., Booth, C. H. & Bridges, F. (1997). *Phys. Rev. B*, **56**, 7993–8000.
- Dallera, C., Krisch, M. H., Rogalev, A., Gauthier, C., Goulon, J., Sette, F. & Sole, A. (2000). *Phys. Rev. B*, **62**, 7093–7097.
- Hämäläinen, K., Siddons, D. P., Hastings, J. B. & Berman, L. E. (1991). *Phys. Rev. Lett.* **67**, 2850–2853.
- Lawrence, J. M., Kwei, G. H., Canfield, P. C., DeWitt, J. G. & Lawson, A. C. (1994). *Phys. Rev. B*, **49**, 1627–1631.
- Lee, P. A., Rice, T. M., Serene, J. W., Sham, L. J. & Wilkins, J. W. (1986). *Comments Cond. Matt. Phys.* **12**, 99–161.
- Malterre, D., Grioni, M. & Baer, Y. (1997). *Adv. Phys.* **45**, 299–348.
- Sekiyama, A., Iwasaki, T., Matsuda, K., Saitoh, Y., Onuki, Y. & Suga, S. (2000). *Nature (London)*, **403**, 396–398.